

## **Modelling tides in the southern Weddell Sea: updated model with new bathymetry from ROPEX**

***Laurie Padman***

*Earth & Space Research, 1910 Fairview Ave. E., Suite 102,  
Seattle, WA 98102-3620, USA.*

***Robin Robertson***

*College of Oceanic & Atmospheric Sciences, Oregon State University,  
104 Ocean Admin Bldg, Corvallis, OR 97331-5503, USA.*

***Keith Nicholls***

*British Antarctic Survey, Natural Environment Research Council,  
High Cross, Madingley Road, Cambridge, CB3 0ET, U.K.*

### **Introduction**

A significant fraction of the total oceanic kinetic energy in the southern and western Weddell Sea is supplied by tidal currents [Robertson *et al.*, 1998: denoted “RPE-98”]. The region of strong tides includes the ocean cavity under the Filchner-Ronne Ice Shelves (FRIS), and the adjacent broad southern continental shelf and upper slope. The spatial distribution of tidal energy was estimated using a finite-difference barotropic ocean model as a prelude to investigating the effect of tides on other processes of general climate and glaciological interest. Tides have been shown to play a significant role in the formation of dense, High-Salinity Shelf Water (HSSW), Weddell Sea Bottom Water (WSBW), and Antarctic Bottom Water (AABW). HSSW formation is enhanced by the working of the winter sea-ice pack by tidal shear and strain, and by the increase in mean open water percentage due to periodic tide-forced ice divergence (see, e.g., Foldvik and Gammelsrød [1988]). WSBW and AABW are formed by the mixing of dense shelf water types with Warm (or “Weddell”) Deep Water Modified Warm Deep Water (WDW and MWDW) at the shelf/slope front: mixing rates increase near locations where baroclinic tides and other internal gravity waves are generated, very often near the shelf break.

Processes under the FRIS are also influenced by tides. The frictional stress caused by tidal currents flowing under the ice shelf causes mixing of the HSSW up to the base of the glacial ice, leading to melting of the ice base and formation of Ice Shelf Water (ISW). This water type is very cold but relatively fresh, and ultimately contributes to WSBW and AABW formation after the ISW leaves the FRIS cavity, flowing primarily through the Filchner Depression, to the shelf break.

Tidal currents are, however, very sensitive to bathymetry, both total water depth (or water column thickness under ice shelves), and bottom slope. Depth data are sparse throughout much of the western and southern Weddell Sea, hence our ability to model tidal currents may be quite poor in these areas. In this paper our primary aim is to show how modelled tidal currents in the southern Weddell Sea are modified by the inclusion of new bathymetric data collected during the Ronne Polynya Experiment (ROPEX), which was carried out from the Royal Navy ice-strengthened hydrographic vessel, *HMS Endurance*, in January and February 1998.

## ROPEX Bathymetry

The area covered by ROPEX includes the northern Ronne Depression and General Belgrano Bank (“GBB”), which have previously been only very poorly sampled (**Figure 1**). Our ability to work in this area in early 1998 was due to an anomalous absence of ice in this region: the northern extent of the open water area is roughly indicated by the northern limit of the cruise track. Other investigators are studying the most likely cause of this sea-ice anomaly: at present the best hypothesis is that the massive polynya was created by a large-scale wind stress anomaly rather than by oceanic processes.

ROPEX provided us with a chance to better define the extent and minimum water depth ( $H_{\min}$ ) of the GBB. Previous data in this region consists of just a single cruise track, suggesting  $H_{\min} \approx 380$  m. In contrast, the *ETOPO-5* gridded data base has  $H_{\min} \approx 10$  m, while *Viehoff and Li* [1995] suggest that  $H_{\min} < 100$  m, although the evidence for this latter estimate is poor. ROPEX confirmed that  $H_{\min} \approx 380$  m, and also showed that the Ronne Depression does not reach the continental slope between the GBB and the coast, but instead is a smaller feature that is isolated to the north from the deep Weddell Basin by a sill about 400 m deep. As yet, however, insufficient data exist to determine whether there exists a “deep” ( $H > 500$  m) pathway from the Ronne Depression to the shelf break to the east of GBB. With the new bathymetry, the GBB appears to be essentially an extension of the western continental shelf, rather than as an isolated feature (“bank”) as shown in previous charts, both *GEBCO-97* and *ETOPO-5*.

## Effect of Revised Bathymetry on Modelled Currents

The full bathymetric data set from *HMS Endurance* has not yet been fully processed. For the present study we constructed a new gridded bathymetry using just a subset of the data, the water depths recorded at the locations of CTD profiles (see **Figure 1**). We will show below how this revised bathymetry affects certain properties of the tidal current field.

Our tidal model [*RPE-98*] is an ocean-only model, *i.e.*, it does not include ocean interactions with a sea-ice pack. *RPE-98* is based on the depth-averaged shallow-water equations and therefore only predicts the barotropic component of the tidal current field. However, the sparse current data from the Weddell Sea suggests that ignoring the baroclinic flow is a reasonable first approximation. The model equations include terms for quadratic bottom friction (which is doubled under the ice shelves to approximate the additional drag due to the rigid ice/ocean interface), lateral viscosity, Coriolis forces, and surface pressure gradients. We model four tidal constituents, two diurnal ( $O_1$  and  $K_1$ ), and two semidiurnal ( $M_2$  and  $S_2$ ). Boundary conditions

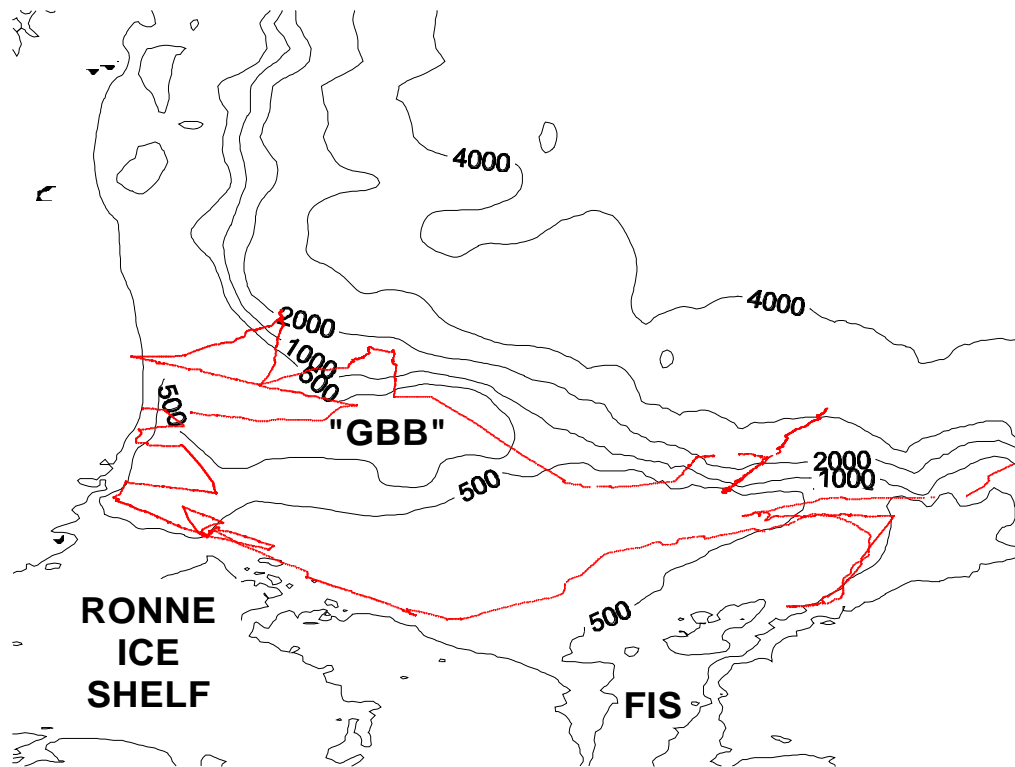


**Figure 1:** Bathymetry in the southern Weddell Sea, revised using ROPEX data (cruise track shown as red dots). Blue dots indicate bathymetry tracklines and point depth measurements from *GEBCO-97*. The General Belgrano Bank (“GBB”), Filchner Ice Shelf (FIS), and Ronne Ice Shelf are indicated.

were obtained from an updated version of the global ocean model described by *Egbert et al.* [1994]. This global model is tuned through inverse methods (“data assimilation”) to benthic tide gauge measurements and sea surface height time series measured by the TOPEX/Poseidon satellite altimeter.

We are primarily interested in tidal currents rather than height fields. The latter vary only slightly when small, local changes are made to the gridded bathymetry. The former, however, are very sensitive to bathymetry. The model response to changes in depth around the GBB differs for the semidiurnal and diurnal constituents, the latter being the most strongly affected. Diurnal tides in this region exist as topographically trapped vorticity waves [*Middleton et al.*, 1987; denoted “*MFF-87*”), whose alongslope propagation characteristics depend on the local across-slope topography. Semidiurnal tides are generally less sensitive to bottom slopes, although their currents still generally increase as water depth decreases. One way to look at the overall impact of changing bathymetry is to plot the “mean” modelled tidal current speed ( $\hat{U}(x,y)$ ), which is evaluated by taking the average current speed (all four tidal constituents added together) from hourly model speed estimates over several spring/neap tidal cycles. We use 45 days of synthesised currents for this calculation. **Figure 2** compares the map of  $\hat{U}(x,y)$  for the bathymetry used by *RPE-98* (“pre-ROPEX”) with the map when the post-ROPEX bathymetry is used. The most significant feature in this comparison is the reduction in modelled  $\hat{U}$  over the GBB, from a maximum value of  $\sim 90 \text{ cm s}^{-1}$ , to  $\sim 30 \text{ cm s}^{-1}$ . Variations in  $\hat{U}$  are also found to the north of the depth-modified region (along the shelf break of the western Weddell Sea), and to the east, along the southern shelf break. (These variations do not show up well in the printed b&w figure, but are clearer in the color figure in the version of this paper that is available online at the ESR web site (<http://www.esr.org>)). Modification of tidal currents outside the region in which the depth grid was altered is due to the change in the tidal energy flux fields, due not only to the steering of the energy flux by topography, but also the change in local energy dissipation. Due to the quadratic bottom drag formulation, the tidal energy dissipation associated with the locally high currents around the GBB, for the *RPE-98* pre-ROPEX bathymetry, is a significant fraction of total energy dissipation in the southern Weddell Sea.

As was stated previously, diurnal tides are more sensitive to bathymetry (both water depth and bottom slope) than semidiurnal tides. An interesting outcome of the analysis by *MFF-87* of shelf/slope moorings near  $74^\circ\text{S}$ ,  $40^\circ\text{W}$  was that the  $K_1$  constituent is much more amplified over the upper slope and outer shelf than the  $O_1$  constituent, even though the large-scale distributions for the two constituents in the Weddell Sea are very similar (see Plate 1 in *RPE-98*). Both constituents were amplified about the same amount in *RPE-98*, i.e., not consistent with the *MFF-87* observations. However, in the model run with post-ROPEX bathymetry,  $K_1$  amplification is greater than for  $O_1$  (see **Table 1**: *MFF-87* major axis values are as listed in *Foldvik et al.* [1990]). While the modelled amplification ratio for the two constituents is not as large as in the data, it does indicate that the ratio arises from bathymetric sensitivity of the topographically trapped barotropic tidal waves rather than from the role of stratification as suggested by *MFF-87*. Note that the bathymetry around the *MFF-87* moorings is the same in both model runs: what has changed is the bathymetry west of the moorings around the GBB and northern Ronne Depression. The change in modelled currents near  $40^\circ\text{W}$  is, therefore, due to the changed propagation of the shelf-trapped modes from the west (these modes have a short along-slope wavelength with energy propagation from west to east, anti-parallel to the direction of phase propagation). The

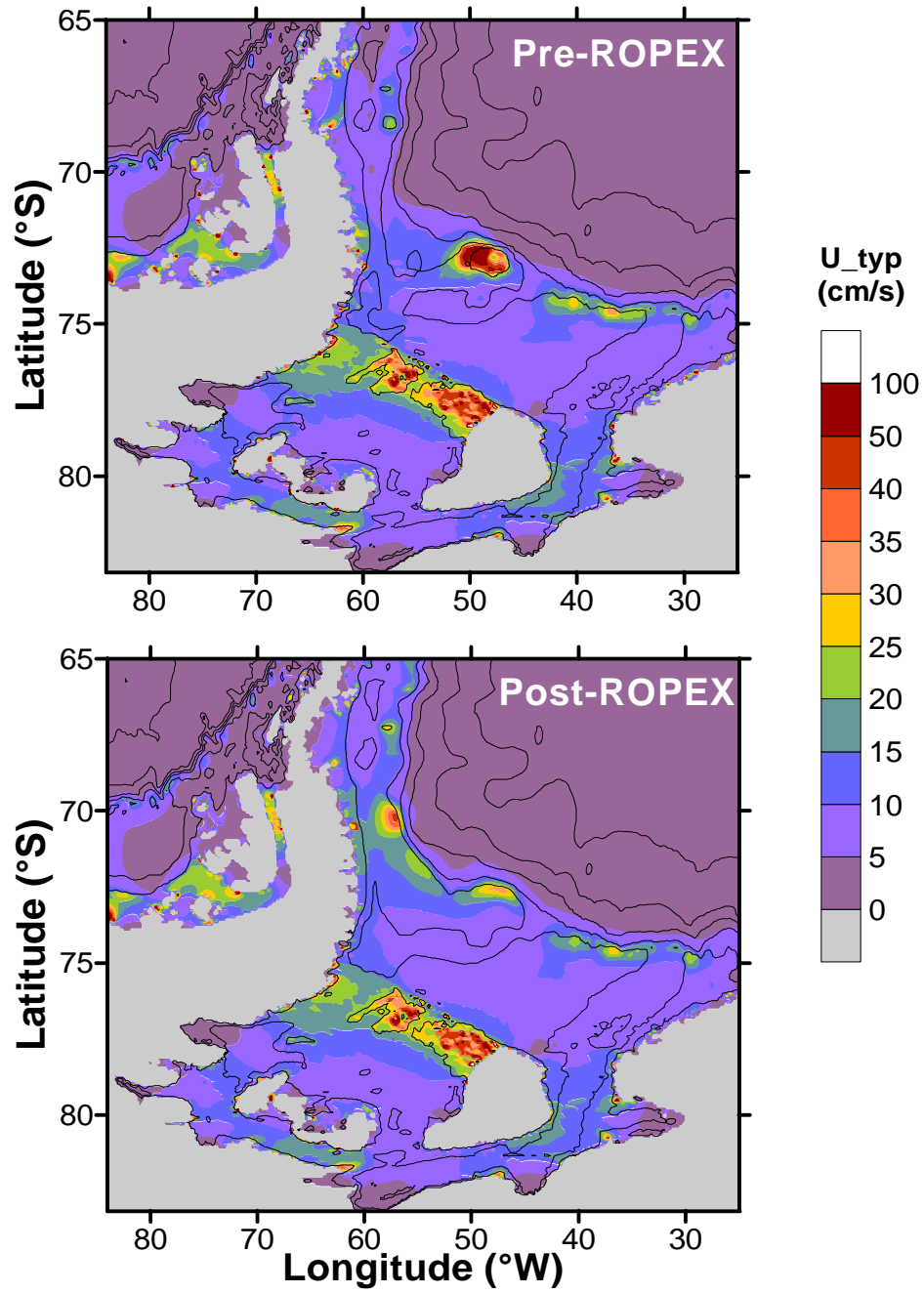


**Figure 2:** Comparison of mean current speeds ( $\hat{U}$ ) from the *RPE-98* barotropic tidal model, for the original *RPE-98* bathymetry (“Pre-ROPEX”, top panel) and the bathymetry revised using data from ROPEX (“Post-ROPEX”, bottom panel).

model run with post-ROPEX bathymetry still overestimates the energy of both diurnal constituents in the *MFF-87* region. This may be an artifact of the smoothness of model topography in a region where detailed surveys demonstrate significant roughness and, therefore, increased dissipation, especially of the topographically constrained shelf/slope modes. Thus, we see that continued improvement of the bathymetric database is necessary not only to model local currents but also to adequately predict to tidal currents “downstream” (in terms of energy propagation) of the region.

**Table 1:** Major axis currents (in  $\text{cm s}^{-1}$ ) for  $O_1$  and  $K_1$  for three moorings on the southern continental shelf (for locations, see *Middleton et al.* [1987] and *Foldvik et al.* [1990]). Shown are measured values, and estimates from *RPE-98* with pre-ROPEX and post-ROPEX bathymetry grids.

Mooring ID	Constituent	Major axis current ( $\text{cm s}^{-1}$ )		
		<i>MFF-87</i>	Pre-ROPEX	Post-ROPEX
<b>A (2000 m)</b>	$O_1$	1.2	6.3	3.4
<b>(slope)</b>	$K_1$	3.7	6.0	6.0
<b>D (400 m)</b>	$O_1$	2.8	16.4	8.9
<b>(shelf)</b>	$K_1$	11.0	16.6	16.9
<b>E (500 m)</b>	$O_1$	2.1	16.8	10.7
<b>(Filchner)</b>	$K_1$	5.1	18.4	18.6

While we are on the subject of energy propagation, note that most of the tidal energy in the western Weddell Sea has previously propagated under the FRIS (see Plate 4 in *RPE-98*). Hence, any attempt to successfully model tidal currents in the western Weddell Sea (*e.g.*, along the Larsen ice front), requires adequate parameterisation of the energy losses under the FRIS. In the present version of the ocean tidal model, energy dissipation under the FRIS is modelled by simply doubling the quadratic bottom drag coefficient to account for frictional losses at the ice/water interface. This is clearly a simplistic view of energy dissipation, which includes not only frictional stress but also any non-elastic deformation of the ice shelf itself by tides. A new study has been proposed to investigate improving the energy loss parameterisations under the shelf ice.

### Tide-Forced Divergence of Sea Ice

It has been recognised for a century or more [*Nansen*, 1898; see p. 180, Volume 1] that sea ice responds to ocean tidal currents by advection and deformation. Our present model does not include a coupled sea-ice cover, however some information on the likely sea-ice response to tidal currents can be obtained by using the model in conjunction with observations of ice pack deform-

ation. It is known that the sea ice in the Weddell Sea diverges periodically in response to the divergence of the stress field at the ice/ocean interface. This divergence is seen in analyses of drift tracks for clusters of ice-mounted, satellite-tracked buoys [Kottmeier *et al.*, 1997; Padman *et al.*, 1998]. These analyses reveal that, over the continental shelf and upper slope, divergence values at tidal frequencies can be as large as those due to wind forcing. In addition, it is believed that tidal-band divergence is a more efficient mechanism than weather-band divergence for increasing the ocean heat loss to the winter atmosphere. This result is due to the greater fluxes that occur through the open water or very thin ice cover than through older, thicker ice. In the tidal “ice accordian”, new open water is created during every divergent phase of the tidal cycle. Thin ice forms (in winter) in the newly opened leads, but can only grow a small amount before the ice pack converges again. The thin new ice cannot resist the convergent stresses, and so is crushed into building ridges at the edges of floes. If the mean ocean heat loss is dominated by heat fluxes through open water, then the reduced net flux through the thickening ice of the floe-edge ridges is unable to offset the increased net flux through the periodically open leads.

For a first approximation to allow us to look at ice divergence in our ocean-only tidal model, the divergence of the sea ice can be approximated by the horizontal divergence ( $\nabla_h(U_{\text{tide}})$ ) of the ocean velocity field. This is the “free drift” assumption, which will only truly apply where the internal ice stresses can be ignored.  $\nabla_h(U_{\text{tide}})$  is comprised of two terms, the surface height gradient and the tidal advection of the water column across varying water depth. The former term is usually insignificant except in very shallow water. The latter term arises from continuity: *e.g.*, if the tidal currents advect a column of water from the 1000 m isobath to the 500 m isobath, conservation of volume requires that the area of the column be doubled. To see how this works in practice, we show in **Figure 3** the deformation of an initially rectangular grid of water particles near the GBB in the original tidal model of *RPE-98*. The locations of the particles are then tracked for 12 h (a half-period of the diurnal tides that dominate over GBB) during spring tides ( $O_1$  and  $K_1$  approximately in phase). Thus, for illustrative purposes, we have chosen an extreme case of tidal divergence. After 12 hours, the array of particles is very distorted. The area of a single cell in the grid can change by up to a factor of five: for an ice cover with no internal ice stresses and perfect coupling to the ocean velocity field, the ice concentration therefore changes by the same amount. Note, however, that the total area of the 11x11-point grid changes by much less than individual elements. The overall grid scale is about 100x100 km, and thus is comparable to the scale of the buoy arrays analysed by Kottmeier *et al.* [1997] and Padman *et al.* [1998]. Thus, we see that the true influence of the ocean tidal divergence on the sea-ice characteristics and ocean/atmosphere fluxes can only be addressed by estimating the length scales over which the free drift approximation is valid, or by incorporating a fully-coupled, realistic ice model in the ocean tidal simulations.

## Summary

Modelled barotropic tidal currents in the Weddell Sea are very sensitive to bathymetry. Updating the *RPE-98* model bathymetry with new depth data obtained during the ROPEX cruise in January and February 1998 results in much lower mean tidal currents over the General Belgrano Bank region, where the largest changes to model water depth were made. Changes in this area also affect tidal currents elsewhere in the Weddell Sea. Currents in the western shelf region, from the sampled area to the tip of the Antarctic Peninsula, are modified by depth changes on the southern

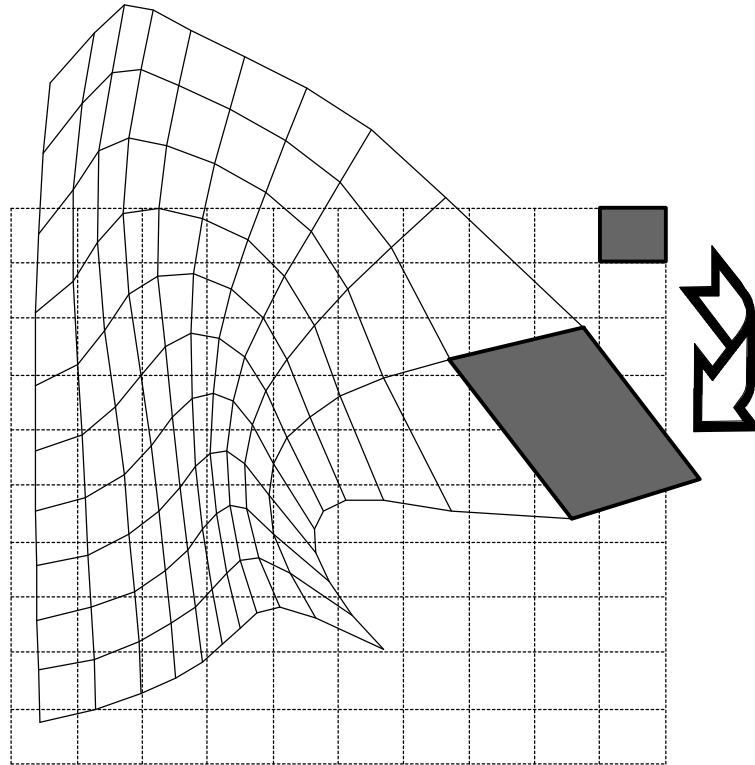


**Figure 3:** Distortion of an initially regular 11x11-element array (about 100 km on a side) centered near the GBB (73°S, 49°W), using the model bathymetry of *RPE-98* (“pre-ROPEX”). The rectangular array represents the grid cells at initialization: the distorted array shows the grid 12 hours later. During this time, particles at each node of the initial grid have been tracked with bicubic interpolation within the time-dependent tide model grid. The period shown represents spring tide, i.e.,  $O_1$  and  $K_1$  currents are approximately in phase. The two shaded cells demonstrate the possible change in area for single cells with length scales,  $L$ , of  $O(10)$  km, whereas the fractional change in area of the entire array is much smaller.

shelf. Predicted currents are also modified along the southern shelf break, notably in the area near 40°W (just west of the Filchner Depression). The new model performs much better here relative to the mooring analyses of *MFF-87*: in particular, the new model predicts the different amplifications for the  $O_1$  and  $K_1$  diurnal constituents, a result which was not obtained with the *RPE-98* pre-ROPEX bathymetry. We expect diurnal energy in this region to be associated with topographically trapped, barotropic vorticity waves, whose energy propagates from west to east. These waves have short wavelengths and thus are very sensitive to bathymetry along their radiation path from the source. Our conclusion is that accurate predictions of tidal currents throughout the southern and western Weddell Sea will depend on additional improvements to the still-sparse depth database for the southwestern Weddell Sea.

Tide-forced divergence of the sea-ice pack is expected to be a significant mechanism for increasing the rate of ocean heat loss to the atmosphere in the austral fall and winter. We find that modelled oceanic horizontal RMS divergences in the tidal frequency bands are comparable to results from analyses of arrays of drifting buoys, with spatial scales of  $O(100)$  km. However, we also find that the modelled RMS divergence values increase significantly as the horizontal length scale is decreased. Since at smaller scales, the interaction of individual ice floes through their internal stresses will increase, these results indicate that the actual influence of ocean tides on RMS divergence of ice must be assessed by using a realistic ice model that is fully coupled to the ocean tidal model.

*Acknowledgements:* The US component of this research was supported by the National Science Foundation grant OPP-9615525. We gratefully acknowledge the assistance of Captain T. Barton, and the officers and crew of *HMS Endurance*, for providing an excellent platform for ROPEX. We also thank Hans Oerter for organising the 13<sup>th</sup> annual meeting of the Filchner-Ronne Ice Shelf Program, and the publication of this Report. Lana Erofeeva and Susan Howard were responsible for much of the tide model running and analysis.

## References

- Egbert, G.D., A.F. Bennett, and M.G.G. Foreman, 1994. TOPEX/POSEIDON tides estimated using a global inverse model. *Journal of Geophysical Research*, **99**, 24,821-24,852.
- Foldvik, A., and T. Gammelsrød, 1988. Notes on Southern Ocean hydrography, sea-ice, and bottom water formation. *Palaeogeography, Palaeoclimatology, and Palaeoecology*, **67**, 3-17.
- Foldvik, A., J.H. Middleton, and T.D. Foster, 1990. The tides of the southern Weddell Sea. *Deep-Sea Research*, **37(8)**, 1345-1362.
- Kottmeier, C., S. Ackley, E. Andreas, D. Crane, H. Hoerber, J. King, J. Launiainen, D. Limbert, D. Martinson, R. Roth, L. Sellmann, P. Wadhams, and T. Vihma, Wind and ice motion statistics in the Weddell Sea, *WMO/TD*, 1/1997, 1997.
- Middleton, J.H., T.D. Foster, and A. Foldvik, 1987. Diurnal shelf waves in the southern Weddell Sea. *Journal of Physical Oceanography*, **17**, 784-791, 1987.
- Nansen, F., 1898. *Farthest North*. George Newnes, Ltd., London.
- Padman, L., C. Kottmeier, and R. Robertson, 1998. Tidal ice motion in the Weddell Sea. Submitted to the *Journal of Geophysical Research*.
- Robertson, R., L. Padman, and G.D. Egbert, 1998. Tides in the Weddell Sea. S. Jacobs and R. Weiss, editors. *Oceanology of the Antarctic Continental Shelf. Antarctic Research Series 75*. American Geophysical Union, Washington, DC.
- Viehoff, T., and A. Li, 1995. Iceberg observations and estimation of submarine ridges in the western Weddell Sea. *International Journal of Remote Sensing*, **16**, 3391-3408.